Structures of regenerated cellulose films revealed by grazing incidence small-angle x-ray scattering*

Fernanda F. Rossetti
Biophysical Chemistry II, Institute of Physical Chemistry and BIOQUANT, University of Heidelberg, INF 253, D-69120 Heidelberg, Germany and Physik-Department, Technische Universität München, LS E22, James-Franck-Str.1, D-85747 Garching, Germany

Panteleimon Panagiotou
Physik-Department, Technische Universität München, LS E13, James-Franck-Str.1, D-85747 Garching, Germany

Florian Rehfeldt[a)]
Physik-Department, Technische Universität München, LS E22, James-Franck-Str.1, D-85747 Garching, Germany

Emanuel Schneck
Biophysical Chemistry II, Institute of Physical Chemistry and BIOQUANT, University of Heidelberg, INF 253, D-69120 Heidelberg, Germany and Physik-Department, Technische Universität München, LS E22, James-Franck-Str.1, D-85747 Garching, Germany

Martin Dommach, Sergio S. Funari, and Andreas Timmann
HASYLAB at DESY, Notkestrasse 85, D-22603 Hamburg, Germany

Peter Müller-Buschbaum
Physik-Department, Technische Universität München, LS E13, James-Franck-Str.1, D-85747 Garching, Germany

Motomu Tanaka[b)]
Biophysical Chemistry II, Institute of Physical Chemistry and BIOQUANT, University of Heidelberg, INF 253, D-69120 Heidelberg, Germany and Physik-Department, Technische Universität München, LS E22, James-Franck-Str.1, D-85747 Garching, Germany

(Received 24 September 2008; accepted 20 November 2008; published 2 February 2009)

The characteristic in-plane length scales of ultrathin films of regenerated cellulose are measured using noncontact atomic force microscopy (NC-AFM) and grazing incidence small-angle x-ray scattering (GISAXS) in ambient atmosphere and under various humidity conditions. The aim is to elucidate the structural basis for the excellent compatibility of cellulose supports to planar lipid membranes. Films are deposited on silicon wafers by Langmuir-Blodgett (LB) transfer and spin coating. NC-AFM height profiles and the resulting calculated power spectral density functions indicate that both kinds of cellulose films have almost identical root-mean-square roughness values (0.7–0.8 nm) and very similar characteristic length scales (32 nm), respectively. GISAXS measurements, both above and below the critical angle of total external reflection, show that the dominant length scales in the bulk and near the surface of the films are comparable (~50 nm). The origin of these length scales can be attributed to the bundle of rodlike molecules of cellulose that result during the regeneration process (i.e., as a consequence of the cleavage of the silyl side chains of trimethylsilylcellulose). Exposure of the cellulose samples to various humidities shows that above a relative humidity of 97% a significant swelling of the films occurs, which is consistent with our previous findings. The swelling of films with more than 30 LB monolayers of cellulose induces a remarkable out-of-plane rearrangement of the cellulose bundles, due to a reduced influence of the solid substrate compared to thinner films with only eight to ten LB monolayers. [DOI: 10.1116/1.3068692]

I. INTRODUCTION

Communications between living cells and their environments are mediated via a variety of poly- or oligosaccharide complexes, such as glycocalix and extracellular matrix (ECM).[1,2] They can maintain high osmotic pressures, generate hydrated "cushions" between cells and tissues, and control the metabolism. One of the promising strategies for quantitative characterization of ECM and glycocalix models is the confinement of hygroscopic polymer films or monolayers of lipopolymers (or glycolipids) at interfaces. To date, grafted films of dextran[3] and poly(ethylene glycol) brushes[4] have been used in numerous fields, due to their good resistance against nonspecific adsorption of proteins.

*This paper was submitted as part of In Focus: Synchrotron Radiation and Neutrons in Biointerface Science.

a)Present address: University of Göttingen, III. Physikalisches Institut, Friedrich-Hund-Platz 1, D-37077 Göttingen, Germany.
b)Author to whom correspondence should be addressed; electronic mail: tanaka@uni-heidelberg.de

Cellulose is not only the main constituent of cell walls of plants but also one of the most important renewable resources in chemical industry.[5] Cellulose consists of a linear chain of $\beta(1\rightarrow4)$-D-glucose. Strong hydrogen bonding between these linear polysaccharides results in semicrystalline fiber structures. For the design of advanced materials, synthetic modification of cellulose has been conducted to introduce various functionalities.[6] Substitution of some hydroxyl protons causes drastic changes in the physical properties: in fact, silylated cellulose derivatives are often soluble in nonpolar solvents due to the significant reduction in the intermolecular hydrogen bonding.[7,8] For example, Wegner and co-workers[9,10] demonstrated that Langmuir monolayers of trimethylsilylcellulose (TMSC) could be transferred onto a hydrophobized substrate by the Langmuir-Blodgett (LB) method. Subsequent exposure to HCl vapor regenerated TMSC to pure cellulose.

In our previous accounts, we demonstrated the excellent suitability of regenerated cellulose LB films for supporting artificial and native cell membranes.[11–14] For example, when an artificial lipid bilayer is deposited onto a semiconductor electrode coated with cellulose, the electric resistance of the "polymer supported" membrane amounts to 0.5 MΩ cm (Refs. 2 and 11) which is 5–50 folds larger than the corresponding values for "solid supported" membranes.[15] We also reported that human red blood "ghost" cells readily spread on regenerated cellulose without loosing their intrinsic structural asymmetry.[12] In contrast to the dissipated membrane patches observed on strong polyelectrolyte films (e.g., polylysine),[12] the cell membranes continuously covered the cellulose surface. Claesson and co-workers also reported a clear difference between the adsorption of polyelectrolytes onto cellulose and that on glass using the surface force technique[16] and x-ray photoelectron spectroscopy,[17] which can be attributed to the steric repulsion exerted by cellulose and the smaller surface charge density on neutral cellulose surfaces. To understand the interfacial forces operating in such ultrathin polymer films, we previously studied the static and dynamic hydration of regenerated cellulose films, prepared by LB deposition and by spin coating.[18] There, we found that the water uptake ability of cellulose is independent of the dry film thickness and the preparation method. However, a systematic study of the local (mesoscopic or nanoscopic) structures of regenerated cellulose films is still missing. Our aim is therefore to get a better understanding of the properties of cellulose films that are important in the context of biological applications, such as uniformity and behavior upon swelling.

In this study, we investigate the dominant in-plane length scales of cellulose thin films in the range of 2–300 nm by combination of a real space imaging technique (noncontact atomic force microscopy, NC-AFM, also called as dynamic force microscopy)[19,20] and an advanced reciprocal space mapping technique (grazing incidence small-angle x-ray scattering, GISAXS).[21–27] The vertical structure of the samples was investigated by x-ray reflectometry. All these techniques are well suited for the characterization of mesoscopic and nanoscopic structures of polymer materials at the interface[21–27] and will allow us to understand the basis of the excellent suitability of cellulose films as supports for native and artificial lipid membranes.

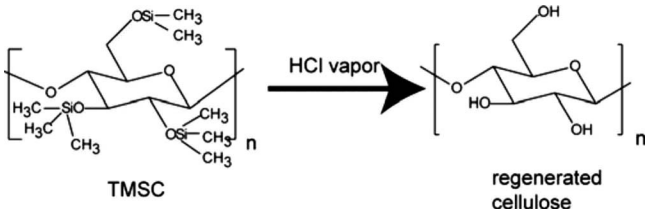

CHART 1. Chemical structures of trimethylsilylcellulose (TMSC, left) and regenerated cellulose (right).

NC-AFM is a noninvasive force microscopy, which possesses a remarkably high sensitivity to local structures in the vicinity of the surface. In contrast to AFM used in contact mode, known as a static mode, that records the z-position of the cantilever by maintaining a constant deflection, NC-AFM enables one to monitor the amplitude of a resonating cantilever. For noninvasive detection and true atomic resolution[20] NC-AFM is performed in the frequency modulation mode.[20,28] The applied tip-sample separation is big and lies in the attractive regime of the Lennard-Jones potential. To avoid contact between tip and sample, the amplitude is kept large, so that the restoring force is bigger than the attractive force.[20] Thus, contrarily to tapping mode AFM,[20] the vibrating tip touches the surface at no time. In fact, our preliminary experiments with contact mode AFM suggested that the surface structure was disturbed during the scanning. In addition to the information on the surface topography obtained by NC-AFM, GISAXS experiments at a synchrotron radiation facility allowed for the measurement of the off-specular x-ray scattering, which reveals the dominant internal structures in polymer thin films in the length scale from ~2 up to ~300 nm. Here, we deposited three kinds of cellulose thin films on silicon wafers—two LB films of different thickness and a spin coated film—and complementarily applied the mentioned characterization techniques. In particular, the samples were measured both above and below the critical angle of total external reflection, which allowed us to be sensitive to both the surface and the bulk of the film. Additionally, the influence of hydration on the structures of the cellulose films was studied by exposing the samples to various humidity conditions and subsequently performing GISAXS experiments. The latter investigation is particularly important in view of biological applications, where the cellulose films are in a fully hydrated state.

II. MATERIALS AND METHODS

A. Materials, sample preparation

Octadecyltrimethoxysilane (ODTMS) was purchased from ABCR (Karlsruhe, Germany). Trimethylsilylcellulose (Chart 1) was synthesized from cellulose powder (M_W ~25.000 g/mol, purchased from Fluka), as reported previously.[9,10,12] The average degree of substitution was es-

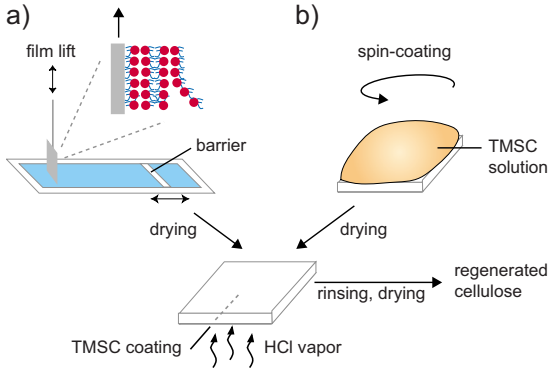

FIG. 1. (Color online) Schematic illustration of the sample preparation methods: (a) Langmuir-Blodgett film deposition and (b) spin coating method.

timated by elemental analysis to be ~2.1. All other chemicals were purchased from Fluka (Munich, Germany), and were used without further purification. Two types of silicon wafers were used as substrates for the deposition of cellulose films. One-side polished, *p*-type boron doped silicon [100] wafers with a thermal oxide layer of about $d=(147\pm5)$ nm were a gift from Wacker Siltronic (Burghausen, Germany) and were used for the AFM experiments, as well as for the GISAXS experiments performed at the A2 beamline (see below). Further silicon [100] wafers with a native oxide layer of ~1 nm thickness were purchased from Si-Mat (Landsbergam Lech, Germany) and used for the GISAXS experiments at the BW4 beamline (see below), as well as for x-ray reflectometry. Each wafer was cut into square pieces (either 60×60 mm^2, or 24×24 mm^2). The substrates were cleaned with acetone and methanol, and sonicated in a mixture of 1:1:5 (v/v) H_2O_2 (30%): NH_4OH (30%): H_2O. They were soaked another 30 min at 60 °C in the same solution, and then rinsed extensively with water (Millipore, Molsheim, France; $R>18$ MΩ cm^{-1}). Subsequently, the cleaned wafers were dried at 70 °C for 1 h, and stored overnight in a vacuum chamber.

A schematic overview of the sample preparation is presented in Fig. 1. Prior to LB deposition [Fig. 1(a)], self-assembled monolayers of ODTMS were grafted onto freshly cleaned wafers to render the surface hydrophobic, showing a static contact angle to a sessile droplet of water $\theta_{H_2O}>95°$.[29] A solution of TMSC dissolved in either chloroform or toluene (concentration of ~0.7 mg/ml) was spread on the water subphase of a self-built Langmuir trough (subphase area: 982 cm^2) at 20 °C. The monolayer was compressed with a barrier speed of 100 μm s^{-1} to a lateral pressure of either 30 mN m^{-1} (when depositing 8 monolayers) or 20 mN m^{-1} (when depositing 10 or 30 monolayers) and transferred onto the hydrophobized substrate.[12,18] Following the successive deposition of 8, 10, or 30 monolayers, the film was dried at 70 °C for 1 h, and stored overnight in a vacuum chamber. The hydrophobic trimethylsilyl side chains were cleaved by exposing the hydrophobic TMSC multilayer (water contact angle $\theta_{H_2O}>70°$) to fuming HCl for 20 s. After rinsing with water and drying the samples, we obtained a hydrophilic ($\theta_{H_2O}\sim35°$), regenerated cellulose film.[12,18] The film thickness was measured by ellipsometry (Plasmos GmbH, Munich, Germany) before (7.8, 7.4, and 27.7 nm for 8, 10, and 30 monolayers, respectively) and after regeneration (4.6, 4.2, and 12.4 nm) using the refractive indices of $n=1.404$ for TMSC and $n=1.505$ for regenerated cellulose, respectively.[10,18] The spin coating of TMSC [Fig. 1(b)] was carried out with a Delta 10 spin coater (B.L.E. Laboratory Equipment GmbH, Singen, Germany).[18] 200 μl of TMSC chloroform solution (1 mg/ml) were deposited onto a silicon wafer, and the substrate was rotated for 10 s at 1000 rpm, and for 90 s at 5000 rpm. After spin coating, the TMSC film was dried at 70 °C and stored in a vacuum chamber. The regeneration of TMSC followed the same protocols described above. The film thicknesses before and after the regeneration were 7.9 and 3.7 nm, respectively. Each of the thickness values presented here is the mean value of more than three independent ellipsometry measurements, showing a small deviation of ±0.2 nm. The decrease in the thickness according to the regeneration (~50%) can be attributed to the cleavage of trimethylsilyl side chains upon the exposure to HCl vapor, as reported previously.[9]

B. Noncontact atomic force microscopy

NC-AFM experiments were carried out in ambient atmosphere at room temperature using an Autoprobe CP AFM (VEECO Instruments GmbH, Mannheim, Germany). To gain topographic images with a high resolution, and to minimize torsion and friction forces[30] a V-shaped silicon nitride (Si_3N_4) cantilever with a high aspect ratio, an asymptotic conical shape (typical curvature radius of the tip of 10 nm) and a spring constant of 3.2 N/m was used (Ultralever, ThermoMicroscopes, Sunnyvale, CA, USA). The measurements were performed close to the eigenfrequency of the tip at a working frequency of 82 kHz in air at ambient conditions. By choosing a rather stiff spring constant of the cantilever and a large oscillation amplitude (10–100 nm) (Ref. 20) we ensured that the restoring force exceeded the adhesion force caused by the adsorbed water layer on the surfaces of the sample and the tip. Noncontact conditions were maintained at a resonance frequency of 82 kHz in air at ambient conditions by adjusting the cantilever oscillation amplitude and the tip-sample distance. Different sample positions were probed. To obtain statistical information on the sample surface, the PSD function was calculated from the two-dimensional (2D) Fourier transformation of the height-height correlation function by the radial average of the isotropic intensity data in Fourier space. Scanning in various scan ranges (from 0.5 up to 20 μm) allows the PSD to cover different intervals in reciprocal space, and enlarge the accessible q-range. Additionally, the PSD provides complementary information to the GISAXS data, since it detects the lateral features only on the sample surface, while the GISAXS can resolve internal structures inside polymeric thin films.

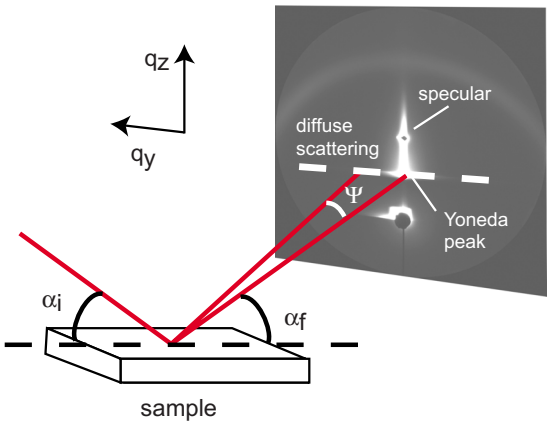

FIG. 2. (Color online) Geometry of the scattering vector components and a typical scattering pattern of a spin coated cellulose film.

C. Grazing incidence small-angle x-ray scattering

GISAXS experiments were carried out at the beam lines A2 and BW4 at HASYLAB (Hamburg, Germany). The comparison of structures present in cellulose films prepared by LB transfer and spin coating was performed at A2, while the studies on the influence of layer hydration and layer thickness were carried out at BW4.

The monochromatic synchrotron beam (A2: $\lambda=1.50$ Å; BW4: $\lambda=1.38$ Å) impinges onto the surface at a fixed angle of incidence α_i, which is either slightly above (here 0.7°) or slightly below (0.13°) the critical angle of total external reflection (that is 0.16° for regenerated cellulose with $\lambda=1.38$ Å), allowing us to gain the internal structures of the polymer thin films. Note that the internal structures of the cellulose films used here can be probed even by illuminating the sample at an incidence angle below the critical angle, because the film thickness is in the same range as the penetration depth of the x rays (3.9 nm for cellulose, with $\lambda=1.38$ Å).

Measurements performed as a function of ambient humidity were carried out by exposing the samples to saturated solutions of KCl (84.3% relative humidity at 25 °C), KNO_3 (93.6%), and K_2SO_4 (97.3%) during the scattering experiment (the equilibration time prior to the measurement was at least 1 h).

The two-dimensional scattering patterns were recorded by a charge coupled device camera (marCCD165, mar research, Norderstedt, Germany) at a distance of either 1.1 m (A2) or 2.3 m (BW4) from the sample. Therefore, a relaxed resolution was achieved that enabled the detection of structures between 2 and 340 nm at A2 and between 3 and >300 nm at BW4. For reducing the background from air scattering, the complete flight path was evacuated. The geometry of the scattering vector components (q_y and q_z) and a typical scattering pattern obtained in this study (spin coated film with a thickness of 3.7 nm) are presented in Fig. 2. The scattering vector component perpendicular to the plane of incidence (q_y) is a function of the out-of-plane (horizontal) scattering angle Ψ at the off-specular conditions $\alpha_i \neq \alpha_f$ and $\Psi \neq 0$:

$$q_y = \frac{2\pi \cos \alpha_f \sin \psi}{\lambda}. \quad (1)$$

The out-of-plane cuts of the scattered intensity as a function of q_y (at constant q_z) were extracted from the 2D detector images by integrating over a stripe of 60 pixels width (i.e., 60 cross sections) immediately above the Yoneda peak (Fig. 2), i.e., in the range $q_z=0.048\pm0.009$ nm^{-1} for $\alpha_i=0.7°$ and $q_z=0.051\pm0.009$ nm^{-1} for $\alpha_i=0.13°$. These integrations were done to improve the signal-to-noise ratio.

D. X-ray reflectometry

X-ray specular reflectivity experiments were carried out at the ID10B beam line at the European Synchrotron Research Facility (ESRF, Grenoble, France), using electrons of either 8 keV ($\lambda=1.54$ Å), or 21 keV ($\lambda=0.59$ Å) energy.

The intensity versus q_z curves that were obtained were fit with the program PARRATT32[31] by using a box model that assumes that the investigated layers in the sample are homogeneous. The theoretical scattering length densities ρ_{SLD} of the materials present at the sample surface (i.e., Si, ODTMS, and cellulose) were calculated according to

$$\rho_{SLD} = \frac{N_A \rho}{M} \times \sum_{i=1}^{n} b_i, \quad b_i = \frac{e^2}{4\pi\varepsilon_0 m_e c^2} f_{1i}, \quad (2)$$

where N_A is the Avogadro number, ρ is the density of the material, M is the molecular weight, b_i is the bound coherent scattering length of the ith atom, e and m_e are the charge and the mass of the electron, ε_0 the permittivity of vacuum, c the speed of light and f_{1i} the first anomalous scattering factor after Henke *et al.*[32] ($f_1=f'+N$; with f'=real part of the anomalous scattering factor defined relative to the nonrelativistic high-energy limit and N=number of bound electrons) of the ith atom.

III. RESULTS AND DISCUSSION

A. Structures of thin LB films (n=8,10) in ambient atmosphere

1. Surface topography by NC-AFM

Figure 3 gives an example of NC-AFM images of a cellulose LB film taken within the scan areas of (a) 5×5 μm^2 and (b) 0.5×0.5 μm^2. The film exhibited no remarkable defects even in a macroscopic area (5×5 μm^2) (a), where the top-to-bottom height deviation remained below 2.0 nm. In fact, the root-mean-square (rms) roughness of the LB film remained constant around 0.8 nm for various different scanning areas (ranging from 0.5×0.5 to 25×25 μm^2) independent of the position probed, confirming the uniformity of the surface topography of the LB film at microscopic and mesoscopic lateral length scales. The measured roughness also agrees well with the very small standard deviation of the film thickness measured by ellipsometry (0.2 nm), where the beam footprint is about 1 mm^2. These results indicate a high uniformity of the regenerated cellulose films in different length scales in terms of both thickness and topography.

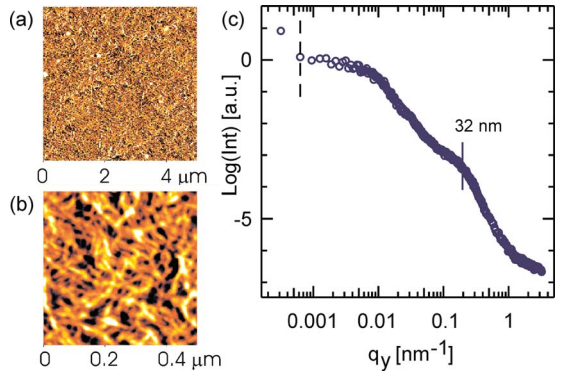

FIG. 3. (Color online) [(a) and (b)] NC-AFM images and (c) the calculated power density spectrum of a thin LB film ($n=8$). (a) Scan size: 5×5 μm^2; z-scale: 1.1 nm. (b) Scan size: 0.5×0.5 μm^2; z-scale: 1.4 nm. For both scan sizes, the top-to-bottom height deviation is less than 2.0 nm and the rms roughness is 0.8 nm. (c) The power density spectrum of a thin cellulose LB film, deduced from radially averaged (2D-) Fourier transformation of the height profiles gained by the NC-AFM measurements (at a scan size of 0.5×0.5 μm^2), points to in-plane structures with a size of 32 nm (solid line). The resolution limit of the experiment is given as a dashed line ($q_y=0.0006$ nm^{-1}).

Since the high-resolution topographic image of the cellulose film [0.5×0.5 μm^2, Fig. 3(b)] suggests the existence of characteristic length scales, we carried out a PSD analysis of the height profiles, in order to obtain their magnitude [Fig. 3(c)]. The obtained intensity (given in arbitrary units) is plotted as a function of the lateral wave vector component q_y. As guide for the eye, the resolution limit of our NC-AFM experiments ($\log[q_y/nm^{-1}]\sim-3.2$) is given as a dashed line. Here, a qualitative analysis—consisting of determining the intersection point of two tangents applied on either side of the curve shoulder in the log(Int.) versus log(q_y) plot—was employed to estimate characteristic length scales of the cellulose films. As indicated by the vertical solid line, a characteristic in-plane length of 32 nm was found for the thin ($n=8$) cellulose films prepared by Langmuir-Blodgett transfer. Recently, Roth *et al.*[33] observed in-plane characteristic length scale of the order of 100 nm in the case of modified cellulose deposited via the LB technique onto glass substrates; although the quantitative assignment of these values to molecular structures seems to be difficult due to the large polydispersity of the original cellulose, both our results and those published by Roth *et al.*[33] remain in the same order of magnitude as the average length of the regenerated cellulose molecules (30–100 nm).

TABLE I. SLD, layer thickness, and roughness of a thin film of cellulose deposited by LB ($n=8$) on a silanized silicon wafer, obtained from fitting the reflectivity curve shown in Fig. 4(a) with a two-layer box model. The energy of the radiation used was 8 keV ($\lambda=1.54$ Å).

	Calculated ρ_{SLD} ($\times10^{-6}$ Å^{-2})	ρ_{SLD} from fitting ($\times10^{-6}$ Å^{-2})	Layer thickness (nm)	Roughness (nm)
Cellulose	13.02	12.6	3.9	1.2
Silane	9.07	7.14	2.0	0.9
Si	20.1	20.1	···	0.6

2. Vertical structure: Specular x-ray reflectometry

X-ray reflectometry was performed to obtain information about the structure of the cellulose films in the direction normal to the layer plane (i.e., in the direction of the scattering vector q_z). Figure 4 shows the x-ray reflectivity curve of a LB sample with $n=8$ measured in ambient atmosphere, together with the corresponding scattering length density (SLD) profile obtained by fitting the data with a box model. The values of the SLD, thickness, and roughness of each layer present at the surface are listed in Table I.

The thickness of the cellulose obtained by reflectometry is in the same range as the value obtained by ellipsometry, although somewhat lower (3.9 vs 4.6 nm). The SLDs obtained from the fitting, on the other hand, agree very well with the theoretical values. The slightly lower than expected value in the case of the silane layer is attributed to the fact that the theoretical SLD value was calculated using the bulk density of ODTMS. Since the density of a self-assembled monolayer is highly influenced by the packing of the molecules, any defects will cause a deviation of the experimental value from the theoretical SLD.

The roughness of the cellulose layer (1.2 nm) is in the same range as both the rms roughness (0.8 nm) and the top-to-bottom height deviation (2.0 nm) measured by AFM, thus confirming the presence of a homogeneous layer on the surface.

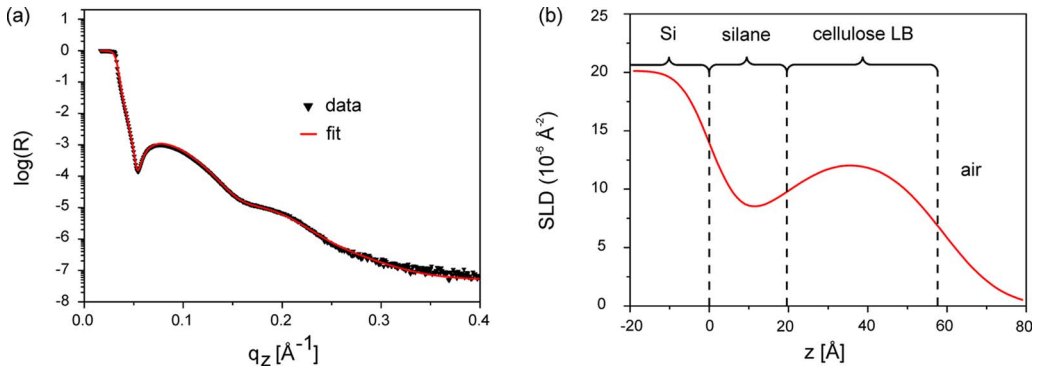

FIG. 4. (Color online) Specular reflectivity (a) and SLD profile (b) of a thin LB film measured in ambient atmosphere ($n=8$).

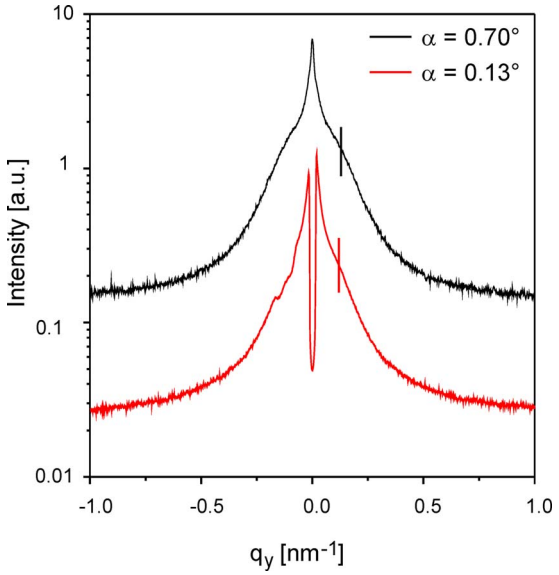

FIG. 5. (Color online) GISAXS out-of-plane cuts of a thin LB film ($n=10$) in ambient atmosphere, measured at two different incidence angles: $\alpha=0.13°$ ($<\alpha_c$ bottom curve) and $\alpha=0.70°$ ($>\alpha_c$ top curve). $\alpha_c=0.16°$ for cellulose. Penetration depth at $\alpha=\alpha_c$: 3.9 nm. The vertical lines correspond to the estimated length scales (46 nm at 0.7° and 50 nm at 0.13°).

From the x-ray data it is furthermore possible to infer that no periodicity along z is present in the cellulose (periodicity would result in a higher amount of fringes in the reflectivity curves). This result is consistent with the findings of Schaub *et al.*,[9] who observed the presence of a periodicity of 1.8 nm for TMSC layers before regeneration, but not for regenerated cellulose. They attributed the phenomenon to a decrease in crystallinity of the cellulose material upon regeneration.[9]

3. Structures near the surface and internal structures: structural characterization by GISAXS

Figure 5 presents the in-plane scattering intensities perpendicular to the plane of incidence (log I vs q_y), which were obtained by GISAXS experiments performed at two angles of incidence, once below (0.13°) and once above (0.7°) the critical angle of total external reflection (which is 0.16° for our samples). A broad shoulder is clearly visible in both GISAXS curves, which indicates the presence of a characteristic lateral length in the cellulose films. It should be noted that quantitative calculation of the structure factor is not possible partially due to the limited range of q_y, ($\sim 0.02-1.1$ nm^{-1}) as well as due to the confinement of polydisperse cellulose molecules within very thin ($d<10$ nm) films. Therefore, instead of assuming a structure factor, we estimated the position of the peak by determining the intersection of two tangents applied to either side of the shoulder in the log(Int.) vs log(q_y) plots. The derived characteristic length scales of the cellulose film at the two different angles are almost identical, i.e., ~50 nm. These reciprocal space results are in good agreement with the values obtained from the PSD analysis of the surface topography in real space (32 nm, gained by NC-AFM at the microscopic scale). It should also be noted that the observation area (i.e., the beam footprint) for GISAXS (width: 400 μm; length: from 33 to 176 mm depending on the angle of incidence) is more than 500 000 times larger than the scan areas in NC-AFM experiments.

The comparable characteristic lengths obtained by NC-AFM and GISAXS strongly suggest that the local film structures are independent of the scan range, and thus confirm the excellent uniformity and reproducibility of the films from microscopic (order of μm^2) to macroscopic scales (order of cm^2). It should also be pointed out that the length scales of ~50 nm we obtained from the surface topography and GISAXS experiments are obviously not originated from the "thickness" of cellulose aggregates as both the film thickness (~4–5 nm) and the observed top-to-bottom height deviation of the films (2 nm) are well below these values.

Further comparison of the intensity versus q_y curves shown in Fig. 5 indicates that the shoulder at $q_y \sim 0.13$ nm^{-1} is more prominent in the data acquired at an incidence angle of 0.7°. This suggests that the observed characteristic lengths scales are more extensively present in the bulk of the cellulose film, rather than at its surface (even though in this case the penetration depth of the x rays below the critical angle is of the same order of the thickness of the sample itself, illumination at 0.13° is still going to be more sensitive to surface structures, compared to the illumination at 0.7°, where information from the whole layer is obtained).

Previously, Schaub *et al.*[9] characterized the structures of LB films of cellulose derivatives by means of specular x-ray reflectivity and polarized FTIR. They reported that rigid (i.e., rodlike) backbones of TMSC tend to align parallel to the direction of the film transfer before regeneration. To verify whether such structural anisotropy existed in our samples after regeneration, we rotated the cellulose-coated substrate by 90 °C around the surface normal and measured GISAXS. No clear sign of structural anisotropy in the regenerated cellulose films could be observed (not shown). This finding can be accounted for by the formation of randomly oriented bundles of cellulose molecules (size: 30–50 nm) by the cleavage of TMS side chains. This is most likely a consequence of the fact that the cleavage of the TMS chains leads to a decrease in the excluded volume per molecule, which, in turn, results in a decrease the film thickness by a factor of about 2. This can cause forces that act upon the cellulose molecules, inducing a random spatial arrangement.

4. Influence of the hydration

Cellulose is known to be a hygroscopic material.[18] Cellulose films exposed to atmospheres with various degrees of relative humidity (RH) are therefore expected to swell to a larger extent, the larger the humidity is. Figure 6 shows the GISAXS out-of plane cuts for a thin cellulose film exposed to relative humidities of 97.6%, 94.6%, and 85.1%, as well as a curve recorded in ambient atmosphere. All measurements were performed both at $\alpha=0.13°$ [below α_c, Fig. 6(a)] and 0.7° [above α_c, Fig. 6(b)]. At $\alpha=0.13°$ no dramatic change in the shape of the curves is observed when the humidity is increased. In particular, the shoulder visible at q_y

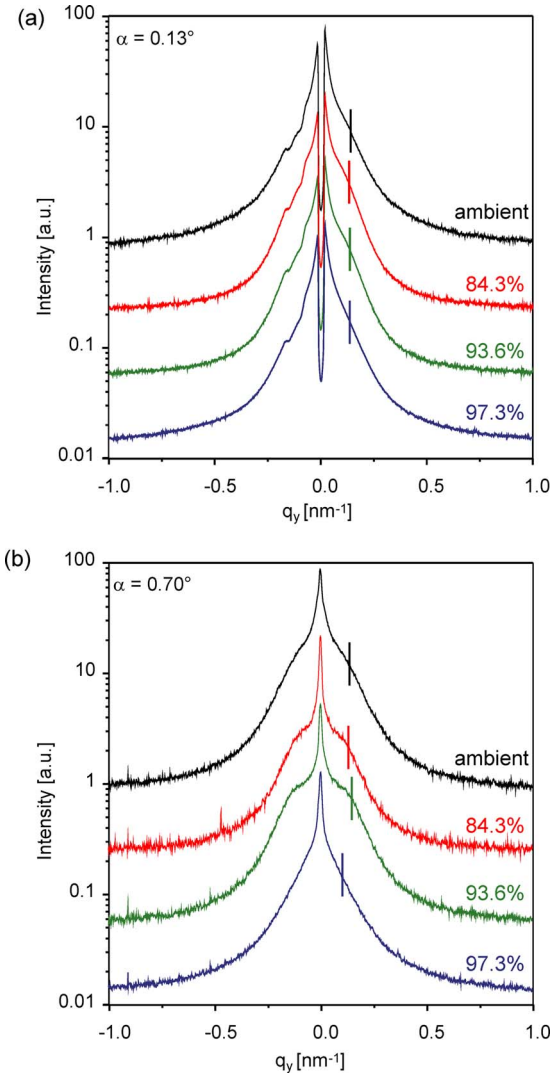

FIG. 6. (Color online) GISAXS out-of-plane cuts of a thin LB film (n=10) measured at α=0.13° (a) and 0.70° (b), under various humidity conditions: ambient, 84.3% relative humidity (in the presence of a saturated solution of KCl), 93.6% RH (KNO_3), and 97.3% RH (K_2SO_4). The vertical lines indicate the position of the shoulders.

$\sim$0.13 nm^{-1} does not shift significantly to lower q_y values (i.e., to larger length scales). It does, however, smoothen out at the highest humidity (RH=97.6%). This "smoothening" can be interpreted as a broadening of the size distribution of the cellulose bundles upon swelling. This could be due to a change in the orientation of some cellulose bundles, which, due to steric constraints, are forced to reorient e.g., more vertically in order to accommodate their increased volume.

Such smoothening of the GISAXS curve at 97.6% RH is even more evident for the curves acquired at α=0.7° [Fig. 6(b)], indicating that the reorienting of the cellulose bundles (and therefore the broadening of the size distribution of the objects that are detected laterally in the cellulose plane) occurs mostly in the bulk of the sample. Furthermore, one has to consider that at high hydration of the film, the contrast in electron density between the swollen cellulose bundles and the remaining amorphous cellulose regions may become lower (due to the high volume content of water in both regions), thus making it harder to resolve characteristic length scales through the GISAXS technique, contributing to the smoothening of the curves.

B. Influence of film thickness

1. Vertical structure: Specular x-ray reflectometry

We have shown above that thin ($\sim$4 nm, n=8–10) films of regenerated cellulose prepared by the LB transfer technique can be considered as homogenous, smooth layers with no vertical structures, but with lateral (i.e., in-plane) structures with a length scale of $\sim$50 nm. In this section we investigate the properties of thick LB films with n=30, i.e., three times as thick as the "thin" cellulose films. Figure 7(a) shows the specular x-ray reflectivity curve for such a sample. Fitting the data with a two-layer box model we obtained the SLD profile, along with thickness and roughness of each layer [Fig. 7(b), Table II]. Again the cellulose layer appears to be homogeneous, with no periodic structures along the z axis. The roughness is slightly higher than for the thin films (1.8 vs 1.2 nm), nevertheless the film can still be considered smooth. The thickness of the cellulose was found to be 10.6 nm, which is in agreement with the value of 12.4 nm obtained by ellipsometry. The SLD is almost identical to the theoretical value (Table II). It is noteworthy how, in this

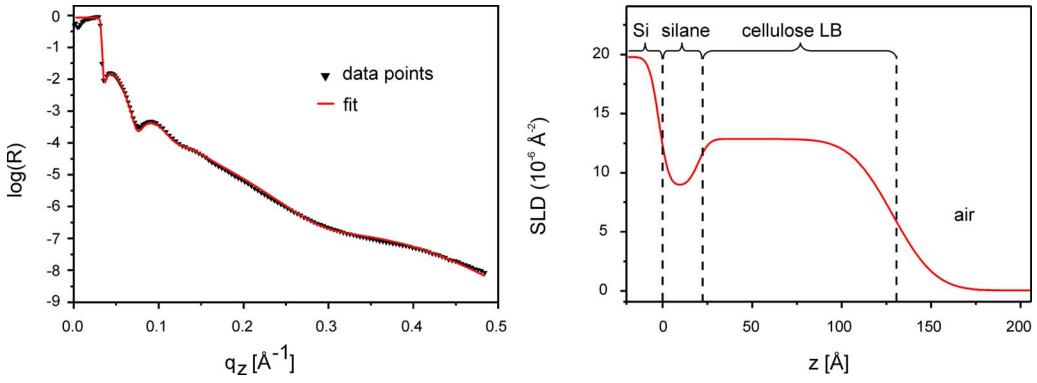

FIG. 7. (Color online) (a) Specular reflectivity and (b) SLD profile of a thick LB film measured in ambient atmosphere (n=30).

TABLE II. SLD, layer thickness, and roughness of a thick film of cellulose (n=30) deposited by LB on a silanized silicon wafer, obtained from fitting the reflectivity curve shown in Fig. 7(a) with a two-layer box model. The energy of the radiation used was 21 keV (λ=0.59 Å).

	Calculated ρ_{SLD} ($\times 10^{-6}$ Å^{-2})	ρ_{SLD} from fitting ($\times 10^{-6}$ Å^{-2})	Layer thickness (nm)	Roughness (nm)
Cellulose	12.97	12.8	10.6	1.8
Silane	9.04	8.87	2.15	0.5
Si	19.8	19.8	⋯	0.4

case, the SLD of the silane is also very close to the theoretical value, suggesting that only very few packing defects are present in the monolayer.

2. Structures near the surface and internal structures: Structural characterization by GISAXS

The GISAXS experiments as a function of incidence angle and relative humidity shown in Fig. 6 for thin cellulose films were repeated for the thick films with n=30 (Fig. 8). At α=0.13° a slight shoulder can be observed at q_y ~0.12 nm^{-1} for the three lowest humidities, which corresponds to a characteristic length scale of 52 nm. At RH =97.6% the shoulder disappears, in a similar fashion as it is observed for the thin cellulose films (Fig. 6). The phenomenon is more evident for the curves recorded at α=0.7°, where also a significant decrease in the width of the peak accompanies the disappearance of the shoulder at the highest humidity. In other words, this means there is a decrease in the scattered intensity at higher q_y (i.e., at about >0.08 nm^{-1}), indicating that smaller structures decrease in number, in favor of an increase in the relative fraction of large structures (>80 nm). This is consistent with a considerable swelling of the cellulose films at RH=97.6% (i.e., up to 70%, as reported previously[18]). However, it should be noted that the phenomenon of peak thinning at is not observed for the thin cellulose layers (Fig. 6), most likely due to the more stringent boundary constraints present in films of <5 nm thickness.

Further comparison of the thick and thin cellulose films (Figs. 8 and 6) shows that the shoulder present at both angles is less prominent in the thick films, suggesting that, already at the lower humidities, there is a wider lateral size distribution of the cellulose structures. This does not only originate from a wider size distribution of the cellulose bundles but also rather from the fact that a larger fraction of the bundles can be arranged in a more vertical or oblique way in the thick films (thus giving rise to a wider range of projected lengths in the film plane), compared to the thin films (where the boundary constraints impose a more in-plane arrangement of the cellulose structures).

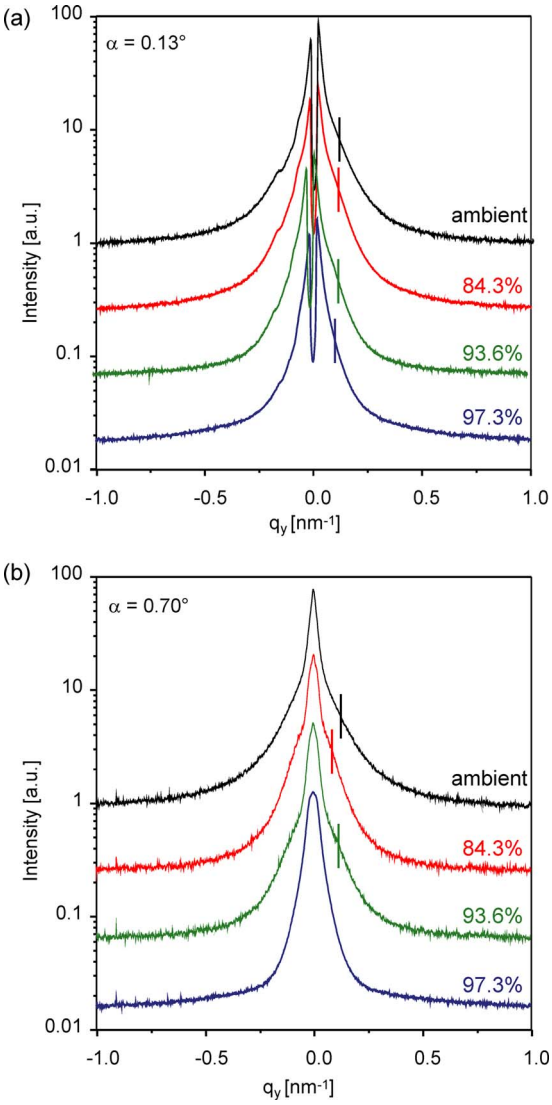

FIG. 8. (Color online) GISAXS out-of-plane cuts of a thick LB film (n=30) measured at α=0.13° (a) and α=0.70° (b), under various humidity conditions: ambient, 84.3% relative humidity (in the presence of a saturated solution of KCl), 93.6% RH (KNO_3), and 97.3% RH (K_2SO_4). The vertical lines indicate the position of the shoulders.

C. Influence of the preparation method

1. Surface topography (NC-AFM)

Representative NC-AFM images of a cellulose film prepared by spin coating are presented in Fig. 9 for two scan areas of (a) 5×5 μm^2 and (b) 0.5×0.5 μm^2. For comparison, the scan sizes and the vertical scale are set the same as the corresponding images in Fig. 3. As can be seen in Fig. 9(a), the topographic image confirms that the spin coated film has no notable defects. Similar to the results from LB films, the rms roughness values (0.7 nm) obtained from different scan areas (ranging from 0.5×0.5 to 25×25 μm^2) are almost identical. Thus, our experimental results confirm that the topographic roughness of regenerated cellulose films is uniform at microscopic and mesoscopic lateral length scales, independently from the preparation methods (i.e., LB or spin coating, see also Fig. 3).

Similarly to the case of LB film, here we also carried out a PSD analysis of the height profiles, in order to extract the magnitude of the length scales [Fig. 9(c), cf. Fig. 3(b)]. Again, a qualitative analysis involving applying tangents on

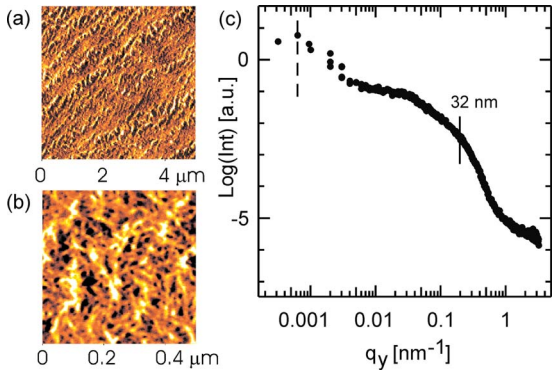

FIG. 9. (Color online) [(a) and (b)] NC-AFM images and (c) the corresponding calculated power density spectrum of a spin coated cellulose film. (a) Scan size: 5×5 μm^2; z-scale: 1.4 nm. (b) Scan size: 0.5×0.5 μm^2; z-scale: 1.4 nm. For both scan sizes, the top-to-bottom height deviation is less than 2.0 nm and the rms roughness is 0.7 nm. (c) The power density spectrum of a spin coated cellulose film, deduced from radially averaged (2D-) Fourier transformation of the height profiles gained by the NC-AFM measurements, points to in-plane structures with a size of 32 nm (solid line). The resolution limit of the experiment is given as a dashed line (q_y=0.0006 nm^{-1}).

either side of the shoulder and determining the position of their intersection was employed to estimate characteristic length scales of these cellulose films, which resulted in a characteristic in-plane length of 32 nm [vertical solid line in Fig. 9(c)]—the same value we obtained for LB films [Fig. 3(c)]. These results indicate that the structures formed by regenerated cellulose are independent of the method used for depositing the films.

2. Vertical structure: Specular x-ray reflectometry

Figure 10 shows the specular x-ray reflectivity curve of a spin coated cellulose sample. Through fitting of the data with a one-layer box model we obtained a thickness of 6.1 nm and a SLD of 7.4×10^{-6} Å^{-2} (Table III). Comparing this thickness with the value obtained by ellipsometry (3.7 nm) it appears that it is much higher than expected, while the SLD is much lower than the theoretical value. We attribute this discrepancy to a smaller density of the spin coated films compared to the films prepared by LB transfer: in fact, if a high volume fraction of air is present in the cellulose layer, then

TABLE III. SLD, layer thickness, and roughness of a thin film of cellulose deposited by spin coating on a silicon wafer, obtained from fitting the reflectivity curve shown in Fig. 10(a) with a one-layer box model. The energy of the radiation used was 8 keV (λ=1.54 Å).

	Calculated ρ_{SLD} ($\times10^{-6}$ Å^{-2})	ρ_{SLD} from fitting ($\times10^{-6}$ Å^{-2})	Layer thickness (nm)	Roughness (nm)
Cellulose	13.02	7.4	6.1	1.1
Si	20.1	20.1	···	0.3

the electron density of the sample is reduced accordingly, leading to a scattering length density that is lower than expected. Furthermore, a density change will affect the refractive index of the sample as well. Since the refractive index is needed to calculate the layer thickness from the ellipsometry data, one can see that an increase in the volume fraction of air in the film will lead to erroneous thickness values.

The roughness obtained by x-ray reflectometry (1.1 nm) is comparable to the one obtained from the NC-AFM measurements (0.7 nm), confirming how a smooth, homogeneous cellulose film can be obtained both by spin coating and LB transfer. In agreement with the results obtained for the LB films, also in this case no periodic structures could be observed along the z axis.

3. Structures near the surface and internal structures

The comparison of Figs. 3 and 9 has shown that the surfaces of spin coated cellulose samples are very similar to those of the samples prepared by LB transfer, exhibiting similar features and a comparable rms roughness. The results obtained by GISAXS for both kinds of substrates at α_i above the critical angle are shown in Fig. 11. The curves appear very similar, indicating that not only the surface structures but also the lateral length scales in the bulk (calculated from the position of the shoulder, i.e., ~50 nm) are identical. This means that the bundles of regenerated cellulose have the same size and are arranged in a similar way for both preparation methods. At q_y above 0.3 nm^{-1}, the scattered intensity of the spin coated samples is slightly lower than in the case

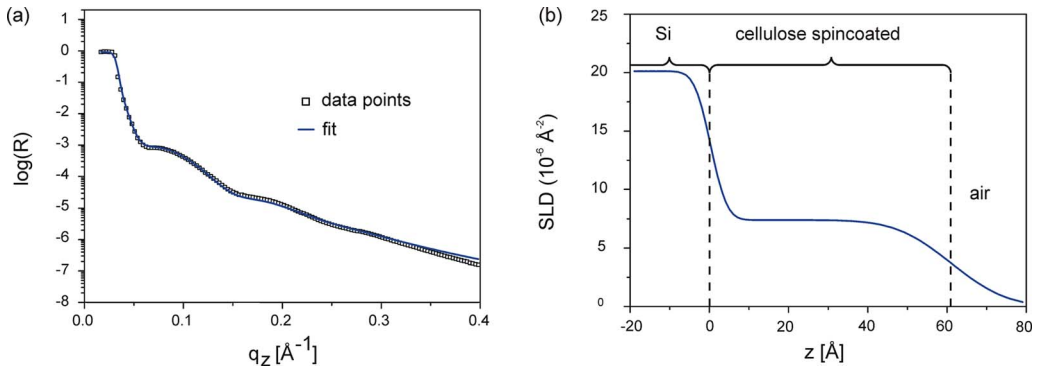

FIG. 10. (Color online) (a) Specular reflectivity and (b) SLD profile of a spin coated film measured in ambient atmosphere.

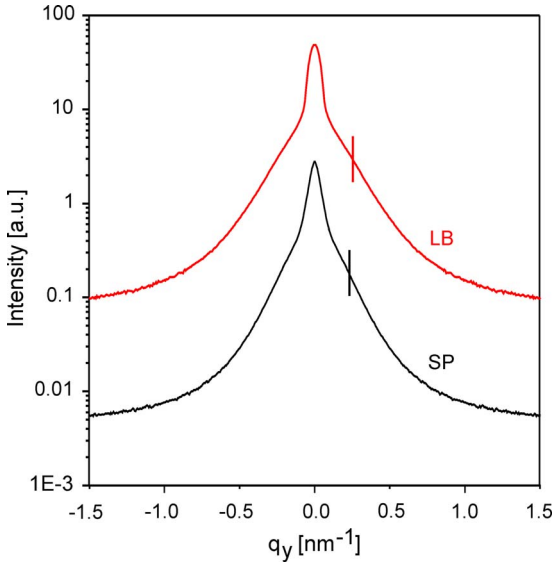

FIG. 11. (Color online) Comparison of the GISAXS out-of-plane cuts of a spin coated film (bottom) and a film prepared by LB transfer (top). The data were measured in ambient atmosphere at an incident angle above the critical angle of total external reflection. The vertical lines indicate the position of the shoulder peaks.

of the LB samples, indicating a lower fraction of the smaller structures. Nevertheless, the overall shape of the two curves remains very similar.

IV. CONCLUSIONS

We studied the local structures of ultrathin, regenerated cellulose films by combination of NC-AFM, x-ray reflectometry, and GISAXS, with the aim of correlating these structures with the excellent suitability of cellulose as a support for native and artificial lipid membranes. Here, three types of cellulose thin films (two LB films of different thickness and a spin coated film) were deposited on silicon wafers. NC-AFM is a noninvasive force microscopy, which possesses a remarkably high sensitivity to the local structures near the surface, while both x-ray reflectometry and GISAXS use synchrotron radiation and are powerful techniques that allowed us to gain both the vertical structure of the thin films (specular x-ray reflectometry) and the dominant in-plane length scales (off-specular x-ray scattering). The rms roughness values of all cellulose films as measured by AFM (0.7–0.8 nm) was found to be independent of the scan area, indicating that the films have a very smooth surface topography. The PSD curves calculated from the Fourier transformation of the height profiles yielded characteristic in-plane length scales that are very similar for both the spin coated films and the films prepared by the Langmuir-Blodgett technique (32 nm). These values agree well with the results gained from GISAXS measured below and above the critical angle of incidence (50 nm). The obtained length scales suggest the formation of bundles of rodlike cellulose molecules resulting from the cleavage of bulky TMS side chains during regeneration. The smoothness of the surface in real space and the homogeneity of surface and internal structures in reciprocal space found in this study confirm the uniformity and reproducibility of cellulose films prepared by both methods in the length scale from microscopic (μm^2) to macroscopic (cm^2). This finding is crucial in explaining why defect-free planar lipid membranes (both native and artificial) are readily formed on cellulose supports. The x-ray reflectometry results, however, seem to point out that spin coated samples are less compact than the LB ones, nevertheless this difference does not seem to influence the quality of the lipid membranes formed on such supports. The experiments performed as a function of humidity indicated that only relative humidities higher than 97% caused a significant swelling of the samples. The swelling induced a rearrangement of the cellulose bundles out of plane, due to steric constraints. This rearrangement was more evident for thicker cellulose films, where the boundary constraints that force the cellulose bundles to remain oriented in-plane in films thinner than 5 nm are not as large. Even though, upon hydration, the cellulose bundles swell by about a factor of 2 and rearrange spatially, the characteristic length scales remain in the same order of magnitude, indicating the great smoothness and uniformity of the films is maintained even under water. Furthermore, the swelling of cellulose has the additional effect of allowing for a looser packing of the films, which is very advantageous when cellulose is used as a cushion to support native membranes, as the hydrophilic parts of transmembrane proteins (such as found in native membranes) can be easily accommodated within the film.

ACKNOWLEDGMENTS

The authors thank HASYLAB at DESY for the beam time at the beam lines A2 and BW4, and Wacker Siltronic for the wafer donation. They thank the ESRF for beam time at ID10B and O. Konovalov for assistance during the experiments. M.T. thanks G. Wegner and E. Sackmann for their helpful suggestions in chemistry and physics of cellulose derivatives. This work has been financially supported by the Deutsche Forschungsgemeinschaft (Contract Nos. DFG Ta 259/6-1 and MU 1487/2-1) and by the Fonds der Chemischen Industrie. F.F.R. was thankful to the DFG for a Postdoc Fellowship under Contract No. Ro 3643/1-1.

[1] H. J. Gabius and S. Gabius, *Glycoscience* (Chapmann and Hall, Weinheim, 1997).
[2] W. D. Comper, *Extracellular Matrix* (Harwood, Academic, Amsterdam, 1996).
[3] S. Löfas and B. Johnson, J. Chem. Soc., Chem. Commun. **21**, 1526 (1990).
[4] J. M. Harris, *Poly(Ethyleneglycol) Chemistry* (Plenum, New York, 1992).
[5] J. F. Kennedy, G. O. Phillips, P. A. Williams, and L. Piculell, *Cellulose and Cellulose Derivatives: Physico-Chemical Aspects and Industrial Applications* (Woodhead, Cambridge, 1995).
[6] D. Klemm, T. Heinze, B. Philipp, and W. Wagenknecht, Acta Polym. **48**, 277 (1997).
[7] J. F. Klebe and H. L. Finkbeiner, J. Polym. Sci. [A1] **7**, 1947 (1969).
[8] D. Klemm and A. Stein, J. Macromol. Sci., Pure Appl. Chem. **A32**, 899 (1995).
[9] M. Schaub, G. Wenz, G. Wegner, A. Stein, and D. Klemm, Adv. Mater. **5**, 919 (1993).
[10] V. Buchholz, P. Adler, M. Backer, W. Holle, A. Simon, and G. Wegner, Langmuir **13**, 3206 (1997).

[11]H. Hillebrandt, G. Wiegand, M. Tanaka, and E. Sackmann, Langmuir **15**, 8451 (1999).
[12]M. Tanaka, S. Kaufmann, J. Nissen, and M. Hochrein, Phys. Chem. Chem. Phys. **3**, 4091 (2001).
[13]M. Tanaka, A. P. Wong, F. Rehfeldt, M. Tutus, and S. Kaufmann, J. Am. Chem. Soc. **126**, 3257 (2004).
[14]M. Tanaka and E. Sackmann, Nature (London) **437**, 656 (2005).
[15]S. Gritsch, P. Nollert, F. Jähnig, and E. Sackmann, Langmuir **14**, 3118 (1998).
[16]E. Poptoshev and P. M. Claesson, Langmuir **18**, 1184 (2002).
[17]O. J. Rojas, M. Ernstsson, R. D. Neumann, and P. M. Claesson, J. Phys. Chem. B **104**, 10032 (2000).
[18]F. Rehfeldt and M. Tanaka, Langmuir **19**, 1467 (2003).
[19]S. Morita, R. Wiesendanger, and E. Meyer, in *Nancoscience and Technology*, edited by P. Avouris, K. v. Klizing, H. Sakaki, and R. Wiesendanger (Springer-Verlag, Berlin, 2002).
[20]E. Meyer, H. J. Hug, and R. Bennewitz, *Scanning Probe Microscopy* (Springer, Berlin, 2004).
[21]T. Salditt, T. H. Metzger, J. Peisl, and G. Goerigk, J. Phys. D: Appl. Phys. **28**, A236 (1995).
[22]J. R. Levine, J. B. Cohen, Y. W. Chung, and P. Georgopoulos, J. Appl. Crystallogr. **22**, 528 (1989).
[23]J. Daillant and M. Alba, Rep. Prog. Phys. **63**, 1725 (2000).
[24]P. Müller-Buschbaum, Anal. Bioanal. Chem. **376**, 3 (2003).
[25]P. Panagiotou, E. Bauer, S. Loi, T. Titz, E. Maurer, and P. Müller-Buschbaum, Z. Kristallogr. **219**, 210 (2004).
[26]M. Rauscher, T. Salditt, and H. Spohn, Phys. Rev. B **52**, 16855 (1995).
[27]V. W. Stone, A. M. Jonas, B. Nysten, and R. Legras, Phys. Rev. B **60**, 5883 (1999).
[28]R. García and R. Peréz, Surf. Sci. Rep. **47**, 197 (2002).
[29]H. Hillebrandt and M. Tanaka, J. Phys. Chem. B **105**, 4270 (2001).
[30]D. Bonnel, (Wiley-VCH, Weinheim, 2000).
[31]L. G. Parratt, Phys. Rev. **95**, 359 (1954).
[32]B. L. Henke, E. M. Gullikson, and J. C. Davis, At. Data Nucl. Data Tables **54**, 181 (1993).
[33]S. V. Roth, G. R. J. Artus, M. Rankl, S. Seeger, M. Burghammer, C. Riekel, and P. Muller-Buschbaum, Physica B **357**, 190 (2005).